

Preparation and characterization of self-assembled nanoparticles based on folic acid modified carboxymethyl chitosan

Yu-long Tan · Chen-Guang Liu

Received: 2 June 2010 / Accepted: 21 March 2011 / Published online: 3 April 2011
© Springer Science+Business Media, LLC 2011

Abstract Folate (FA) modified carboxymethyl chitosan (FCC) has been synthesized and the hydrogel nanoparticles can be prepared after the sonication. Formation and characteristics of nanoparticles of FCC were studied by fluorescence spectroscopy and dynamic light scattering methods. The critical aggregation concentration value of FCC in water was 9.34×10^{-2} mg/ml and the mean hydrodynamic diameter of particle was 267.8 nm. The morphology of nanoparticles was observed by transmission electron microscopy which had spherical shape. Loading capacity (LC), loading efficiency (LE) and the in vitro release profiles of nanoparticles were investigated by doxorubicin (DOX) as a model drug. When the initially added amount of DOX versus the constant amount of FCC polymer was increased, the LC in the nanoparticles was gradually increased and the LE decreased. The in vitro release profile of the DOX from the FCC nanoparticles exhibited sustained release. Cellular uptake of FCC nanoparticles was found to be higher than that of nanoparticles based on linoleic acid (LA) modified carboxymethyl chitosan because of the FA-receptor-mediated endocytosis, thereby providing higher cytotoxicity against Hela cells.

1 Introduction

Colloidal systems such as micelles, liposome, nanoemulsion, polymeric nanoparticles have found numerous applications for delivery of pharmaceutical compounds,

because they can be used to improve the therapeutic index of drugs by modifying their distribution and thus increasing their efficacy and/or reducing their toxicity. Among these colloidal systems, polymeric hydrogel nanoparticles have gained considerable attention owing to their unique potentials via combining the characteristics of hydrogel system with nanoparticles [1]. Hydrogel nanoparticles (HPs) based on natural and synthetic polymers have become an important area of research in field of drug delivery. As natural polymer, polysaccharide have been studied extensively for preparing of HPs because of their biodegradability, lack of toxicity, stability, biochemical activity, and biocompatibility. Several methods have been developed to prepare HPs based on polysaccharides by four mechanisms, namely covalent crosslinking, ionic crosslinking, polyelectrolyte complexation and self-assembly hydrophobically modified polysaccharides [2].

In recent years, self-assembled polysaccharides HPs have been of particular interest because of their self-aggregating characteristics. Hydrophilic polysaccharides have been modified by hydrophobic molecular to produce amphiphilic polysaccharides, which are able to spontaneously form HPs via undergoing intra- and/or intermolecular association between hydrophobic moieties in aqueous environment. Some hydrophobic groups not only help stabilize the structure of HPs by formation of hydrophobic domains, but also endowed nanoparticles novel properties [2]. For example, fluorescein isothiocyanate (FITC), a widely used hydrophobic fluorescein, can be conjugated onto hydrophilic polysaccharides form fluorescence labeling HPs [3, 4]; Na et al. introduced vitamin H to pullulan acetate and prepared corresponding self-assembled nanoparticles (~100 nm) in order to improve their cancer-targeting activity and internalization [5]; Park et al. described *N*-acetyl histidine-conjugated glycol chitosan

Y. Tan · C.-G. Liu (✉)
College of Marine Life Science, Ocean University of China,
Qingdao 266003, People's Republic of China
e-mail: liucg@ouc.edu.cn

self-assembled nanoparticles as a promising system for intracytoplasmic delivery of drugs [6].

Folate (FA) is a vitamin with very low solubility in water (0.0016 mg/ml (25°C)) and displays extremely high affinity to its receptor. Folate-receptor (FR), a glycosyl-phosphatidylinositol (GPI) anchored cell surface, has been known to be overexpressed in several human tumors including ovarian and breast cancers, while it is highly restricted in normal tissues [7]. So, FA has been popularly employed as a targeting moiety of a wide array of drug delivery vehicles including liposomes, protein toxins, polymeric nanoparticles, linear polymers, and dendrimers to avoid their non-specific attacks on normal tissues as well as to increase their cellular uptake within target tumor cells [8–14]. In particular, FA-graft-chitosan has been prepared for DNA and nitric oxide delivery [15, 16], but there are no reports on nanoparticles prepared from FA modified chitosans. We suppose that FA is not only as targeting moiety, but also as hydrophobic groups due to its low water solubility. To investigate this hypothesis, FA was conjugated to amino groups of carboxymethyl chitosan (CMCS) as hydrophobic segments and a targeting moiety. Transmission electron microscopy (TEM) and $^1\text{H-NMR}$ spectra were used to determine the physicochemical structure of the particle, and dynamic light scattering (DLS) was used to determine the size of nanoparticles.

In this study, doxorubicin (DOX) is selected as a drug model. Doxorubicin is an effective and widely used chemotherapeutic agent in different cancers. Despite the success of DOX against many cancers, its short biological half life, nonspecific distribution leading to intolerable adverse effects and development of drug resistance have limited its success. Several polymer based delivery systems developed for DOX are mostly designed to reduce or alter toxicity [17–19]. Therefore, the usefulness of nanoparticles as a carrier of DOX was evaluated by measuring their loading efficiency (LE), drug release profile, cytotoxicity and cellular uptake of nanoparticles *in vitro*.

2 Materials and methods

2.1 Materials

Carboxymethyl chitosan (CMCS, deacetylation degree = 90%, substitution degree of carboxymethyl $\geq 80\%$, and viscosity = 600 mpa s) was obtained from Qingdao Heppe Biotechnology, Ltd (China), 1-ethyl-3-(3-dimethylamino-propyl) carbodiimide (EDC), *N*-hydroxysuccinimide (NHS), triethylamine (TEA), linoleic acid (LA), dicyclohexylcarbodiimide (DCC), DOX, FITC and FA were purchased from Sigma Chemicals. All other chemicals used in this study were of analytical grade.

2.2 Preparation of linoleic acid modified carboxymethyl chitosan (LCC) and FA modified carboxymethyl chitosan (FCC)

Linoleic acid can be coupled to CMCS by the formation of amide linkages through the EDC-mediated reaction as described in our previous study [17]. Briefly, CMCS (1 g) was dissolved in 1% (w/v) aqueous solution (100 ml) and diluted with 85 ml methanol. Linoleic acid was added to the CMCS solution at 0.54 mol/mol glucosamine residue of CMCS followed by drop wise addition of 15 ml EDC methanol solution (0.07 g/l) while stirring at room temperature. 1:1 mol ratio of EDC to LA was used in this study. After 24 h, the reaction mixture was poured into 200 ml of methanol with stirring. The precipitated material was filtered, washed with distilled water, methanol, and ether and then dried under vacuum for 24 h at room temperature [20, 21].

0.2 g of FA dissolved in 10 ml of dimethylsulfoxide (DMSO) was activated by 0.1 g of NHS and 0.2 g of DCC at room temperature for 12 h until FA was well dissolved (FA/NHS/DCC molar ratio=1:2:2). It was then added to a solution of 1% (w/v) CMCS in buffer (pH 4.7). The resulting mixture was added EDC (CMCS/FA/EDC molar ratio=1:1:1) and stirred at room temperature in the dark for 16 h. It was brought to pH 9.0 by drop wise addition of diluted aqueous NaOH and dialyzed first against phosphate buffer pH 7.4 for 1 day and then against water for 1 day. The polymer was freeze-dried. $^1\text{HNMR}$ spectra was measured on a spectrometer (Bruker ARX 300 USA) at room temperature. After stirring for 5 h at room temperature FCC (5 mg) were dissolved in 0.5 ml DMSO [22].

2.3 Preparation of FCC and LCC self-assembled nanoparticles

The modified CMCS was suspended in PBS (pH 7.4) at 37°C for 24 h and sonicated by using a probe type sonifier (Ultrasonic Homogenizer UH-600) at 20 W for 3 min. The sonication was repeated twice to get an optically clear solution by using pulse function (pulse on, 10.0 s; pulse off, 2.0 s). The clear solution of nanoparticles was filtered through a filter (Whatman) to remove dust. Solutions of different concentrations were obtained by diluting the 1% (w/w) stock solution with PBS buffer.

2.4 Measurement of fluorescence spectroscopy

Pyrene, used as a hydrophobic probe, was purified by repeated recrystallization from ethanol and vacuum-dried at 20°C. Purified pyrene was dissolved in pure ethanol (analytical reagent, Sigma) at the concentration of 0.04 mg/ml. About of 20 μl of the result in solution was

added into a 20 ml test tube and the ethanol was evacuated under purging of nitrogen gas. Four milliliters of HD nanoparticles solution was subsequently added to the test tube, resulting in a final pyrene concentration of 1.0×10^{-6} M. The concentration of nanoparticles in the solution ranged from 1×10^{-4} to 1 mg/ml. The mixture was incubated for 3 h in a water bath at 65° and shaken in a SHA-B shaking water bath (GuoHua company, Hebei, China) overnight at 20°. Pyrene emission spectra were obtained using a Shimadzu RF-5301PC fluorescence spectrophotometer (Shimadzu Co., Kyoto, Japan). For measurements of intensity ratios for the third and the first peaks (I_3/I_1) in the emission spectra for pyrene, the slit openings for excitation and emission were set at 15 and 1.5 nm, respectively. The excitation (λ_{ex}) and emission (λ_{em}) wavelengths were 343 and 390 nm, respectively. The spectra were accumulated with an integration time of 3 s/nm [23].

2.5 Transmission electron microscopy (TEM)

Specimens were prepared by dropping the sample solution onto a copper grid. The grid was held horizontally for 20 s to allow the molecular aggregates to settle and then at 45° to allow excess fluid to drain for 10 s. The grid was returned to the horizontal position, and one drop of 2% phosphotungstic acid was added to give a negative stain. The grid was then allowed to stand for 30 s to 1 min before the excess staining solution was removed by draining as above. The specimens were airdried and examined using a Philips EM 400 transmission electron microscope (Netherlands) at an accelerating voltage of 80 kV.

2.6 Particle size distribution

The average particle size and size distribution were determined by quasielastic laser light scattering with a Malvern Zetasizer (Malvern Instruments Limited, United Kingdom). Nanoparticle distilled water solutions of 3 ml (1 mg/ml) were put into polystyrene latex cells and measured at a detector angle of 90°, a wavelength of 633 nm, a refractive index of 1.33, a real refractive index of 1.59, and a temperature of 25°C.

2.7 Preparation of DOX-loaded nanoparticles (FCC-DOX or LCC-DOX)

The same amount of DOX was added to 1 ml 0.1 mg/ml nanoparticles in such a way that 2 ml FCC(or LCC) nanoparticles (1 mg/ml) was added to the solutions of different amounts of DOX (equivalent DOX concentration :100, 200, 400, 500, 800 μ g/ml) while stirring and stored in a dark place for 24 h. The excess DOX, which was not

incorporated into the nanoparticles, was removed by ultrafiltration by using a membrane filter with molecular weight cut-off at 1.0×10^4 (Amicon, USA). Ultrafiltration was repeated until the 490 nm intensity of the filtrate was zero. DOX-loaded nanoparticle solution was added to acetic acid in the final concentration (1%), and the 490 nm intensity of DOX was measured.

The loading capacity (LC) of nanoparticles and DOX LE were calculated by using following equation:

$$LC = (A - B)/C \times 100 \quad LE = (A - B)/A \times 100$$

A = total amount of DOX in added solution; B = total amount of DOX in supernatant after ultrafiltration; and C = weight of the nanoparticles measured after freeze-drying.

2.8 In vitro release study

Folate modified carboxymethyl chitosan-DOX nanoparticles were dispersed in PBS (pH 7.4). The solution containing the nanoparticles and the drug was placed into a cellulose membrane dialysis tube. The dialysis tube was placed in 20 ml of PBS buffer and gently shaken at 37°C in a water bath at 100 rpm. At various time points, the medium was refreshed. Samples were taken a predetermined times from the medium outside of the dialysis, and their DOX concentrations were determined measured UV spectrophotometry at $\lambda = 480$ nm.

2.9 Preparation of FITC-labeled FCC (or LCC) conjugates

To label the FCC (or LCC) conjugates with FITC, FCC (or LCC) conjugate (0.5 g) was suspended in 100 ml of bicarbonate buffer (0.1 M Na_2CO_3 , 0.1 M NaHCO_3 , pH 9.5), 50 mg FITC in absolute ethanol at the concentration of 5 mg/ml was added, and the suspension was magnetic stirred for 24 h at room temperature. The reaction mixture was sonicated three times with the sonifer to obtain FITC-loaded FCC nanoparticles (FITC-FCC). Then the nanoparticles suspension was dialyzed for 3 days against 20% ethanol with three separate exchange of medium to remove unlabeled FITC. The final FITC-labeled FCC conjugates were obtained by freeze-drying. The experiment was protected form light and the obtained labeled FCC conjugates was stored in dark.

2.10 Cellular uptake and cytotoxicity

HeLa cells were seeded into 96-well black plates (Costar, IL, USA) at 4×10^3 cells/well and cultured in 200 μ l RPMI-1640 at 37° in 5% CO_2 until 80% confluent. The cultured medium was changed with fresh medium that

contained FITC-labeled nanoparticles at a particle concentration of 0.05–0.2 mg/ml. At predefined time periods of incubation at 37°, the suspension was removed and the wells were washed three times with 50 µl of PBS to eliminate traces of nanoparticles left in the wells. After that, 50 µl of 0.5% Triton X-100 in 0.2 N NaOH was added to the sample wells to lyse the cells. The fluorescence intensity of each sample well was measured by fluorescence microplate reader (FL600, Bio-Tek, USA) with excitation wavelength at 495 nm and emission wavelength at 520 nm.

To study cellular uptake via fluorescence microscopy, cell suspension (4×10^3 cells/ml, 1 ml/well) were cultured in 6-well cultureplates containing 18 mm coverslips for 24 h. Then the culture medium was replaced by HBSS and pre-incubated at 37° for 0.5 h, and then changed with FITC-FCC suspension (0.2 mg/ml in HBSS). After 1–4 h of incubation at 37°, the cells were washed three times with ice-cold PBS, and the coverslips were put on slides and viewed by fluorescence microscopy.

HeLa cells (human epithelioid cervical cancer cell line) were routinely cultured in RPMI-1640 medium containing 10% heat-inactivated fetal bovine serum (FBS) and 1% penicillin–streptomycin at 37°C, 5% CO₂ and 95% humidity. Cell viability was determined using an MTT assay. We used the DOX-loaded LCC nanoparticles (LCC-DOX) as the control to show FA-receptor-targeted anticancer therapy of FCC-DOX. HeLa cells were incubated in conditioned media containing different concentrations of nanoparticles, FCC-DOX, LCC-DOX or free DOX solution, in 96-well microplates at 37°C in a humidified atmosphere containing 5% CO₂. After predetermined incubation periods, MTT solution was added to each well. After 4 h of incubation at 37°C, the medium was removed and any formazan crystals formed were solubilized with DMSO. After slow shaking for 5 min, the absorbance of each well was determined at 490 nm using a Microplate Reader. The cell viability was expressed as a percentage compared to a control (only test cells were added).

3 Results and discussion

3.1 Preparation of FCC

Folate modified carboxymethyl chitosan was synthesized through the reaction between the carboxylic groups of FA and the amino groups of CMCS. The final product is shown in Fig. 1. The reaction mixture was extensively dialyzed against distilled water and dried to obtain FCC conjugate as a yellow powder. The ¹H NMR spectra of FCC (Fig. 2) showed the presence of the signal of chitosan backbone at 2.0, 2.9, 3.4–3.7 and 4.2–4.6 ppm

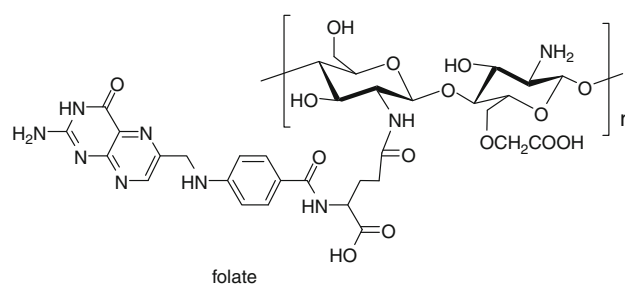


Fig. 1 The structure of FCC

owing to the acetyl group of chitosan and carbon 2, 3–6 and 1 of chitosan. The peaks at 6.6, 7.6 and 8.6 ppm were attributed to the pendant groups of FA, respectively. The degree of substitution (DS, %) value was determined from the relative ratio of the peak area of carbon 12/16 at 6.63 ppm (FA) and the peak area of carbon 5 of FA-CMCS at 3.51 ppm, as seen in Fig. 2. We could get the value (12%) of DS after reaction.

3.2 Aggregate formation of FCC

In order to study the formation of aggregates in a solution of FCC, fluorescence measurements were used to detect the emission spectra of pyrene in the solution. Pyrene was chosen as the fluorescence probe because its condensed aromatic structure is sensitive to polarity. There are five peaks in the spectra of pyrene, the variation in the ratio of intensity of first (372 nm) to third (383 nm) vibronic peaks I_{372}/I_{383} , the so-called polarity parameter, is quite sensitive to the polarity of microenvironments where pyrene is located. A bigger I_{372}/I_{383} value means a greater polarity of the solution around pyrene. Therefore, the formation of the aggregates with a hydrophobic inner core can be detected by means of plotting I_{372}/I_{383} versus polymer concentration. The change of the intensity ratio is shown in Fig. 3. For FCC at lower concentration, I_{372}/I_{383} values remain unchanged, are close to that of pure water (1.7) for there are few aggregates formed. Further increasing concentration, the intensity ratio start to decrease, implying the onset of aggregate from FCC. The critical aggregates concentration (CAC) is 9.34×10^{-2} mg/ml determined by the interception of two straight lines. The CAC is which is lower than CMC of low molecular weight surfactants implying the stability of aggregates from FCC at dilute conditions.

3.3 Size and size distribution and TEM morphology of nanoparticles

The morphological characteristics of nanoparticles were examined using TEM. The TEM image of nanoparticles with the DS% of 2.0% was shown in Fig. 5, which revealed

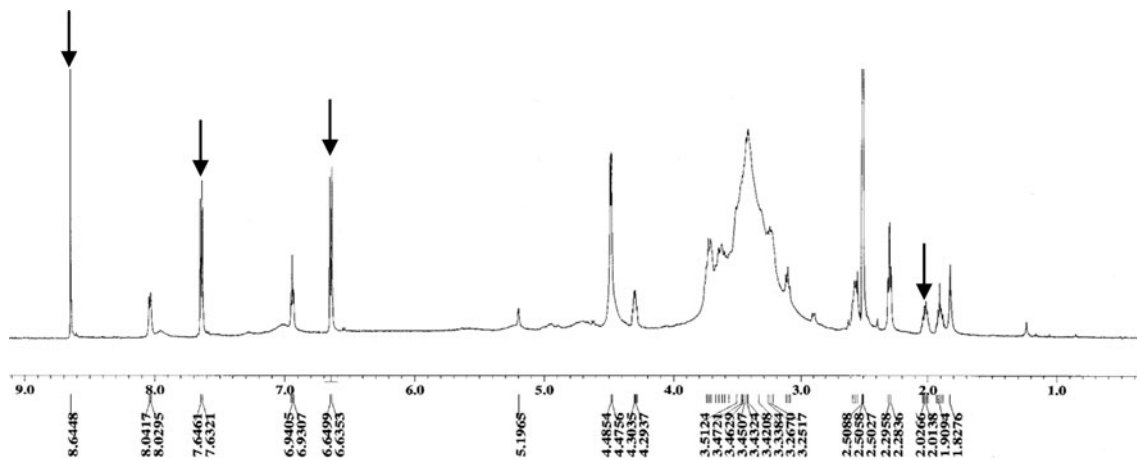


Fig. 2 The spectra of ¹H-NMR of FCC

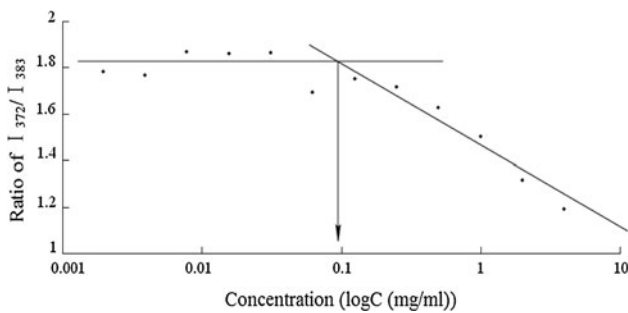


Fig. 3 Plot of the intensity ratio of I_{372}/I_{383} from excitation vs $\log C$ of nanoparticles. CMC of FCC = 9.34×10^{-2} mg/ml

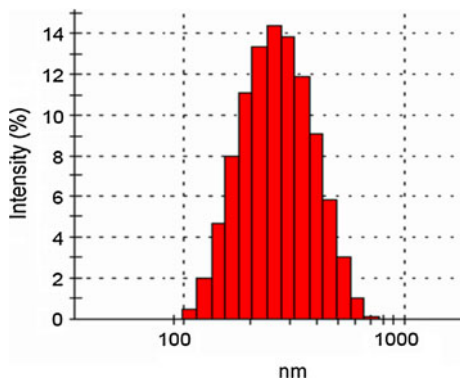


Fig. 4 Size and size distribution of FCC nanoparticle

intact and well-separated, spherical nanoparticle structures. The hydrodynamic diameter of the nanoparticles and its distribution measured by a laser light scattering technique are shown in Fig. 4. The mean hydrodynamic diameter of particle was 267.8 nm.

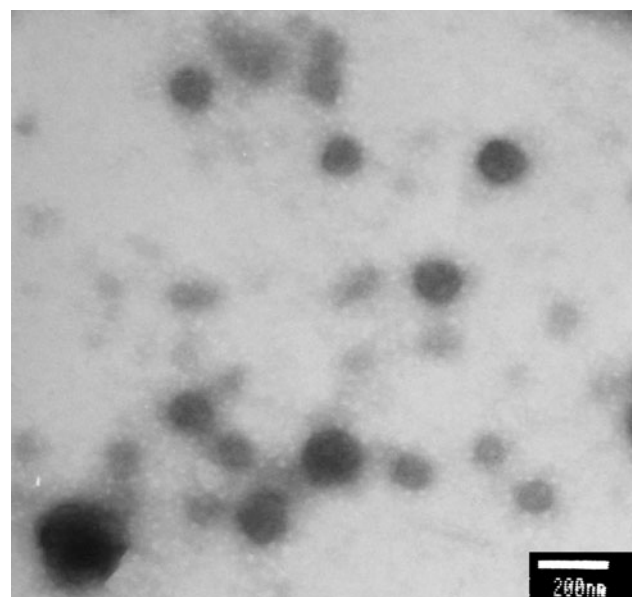


Fig. 5 Transmission electron micrograph of self-aggregates based on FCC

3.4 Drug loading efficiency and encapsulation efficiency

As seen in Table 1, we used varying initial feed weight ratios of DOX to copolymer, ranging from 0.1:1.0 to 0.8:1.0. When the initially added amount of DOX versus the constant amount of polymer (1 mg) was increased, the LC in the nanoparticles was gradually increased from 4.59 ± 0.02 to $28.81 \pm 0.05\%$. On the other hand, the LE decreased from 91.78 ± 0.39 to $72.04 \pm 0.13\%$.

The amphiphilic polymers composed of a hydrophilic segment and a hydrophobic segment can self-assembled in such a way that the hydrophilic part is oriented outside, while the hydrophobic part is buried in the core. These structures have been used to solubilize hydrophobic drugs

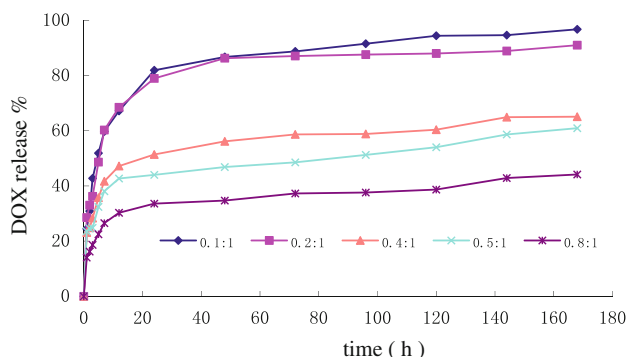
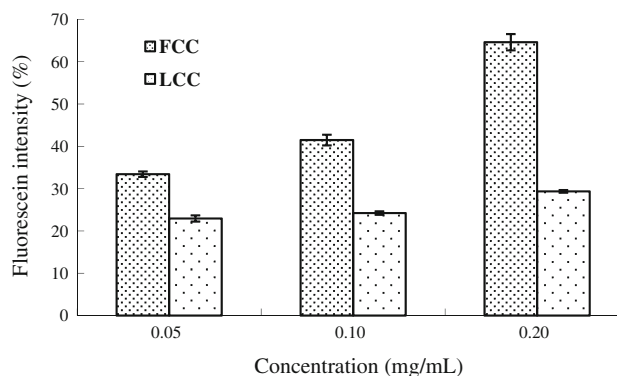
Table 1 DOX loading capacity (LC) and loading efficiency (LE)

DOX (mg)	LE (%)	LC (%)
0.1	91.785 ± 0.39	4.589 ± 0.02
0.2	85.791 ± 0.70	8.579 ± 0.07
0.4	77.407 ± 0.68	15.482 ± 0.14
0.5	72.228 ± 0.28	18.057 ± 0.07
0.8	72.037 ± 0.13	28.815 ± 0.05

inside the core, such as paclitaxel and DOX. We synthesized a FCC conjugate to form nanoparticles that solubilized and stabilized hydrophobic DOX molecules in aqueous solution.

3.5 In vitro release studies

Figure 6 shows the in vitro release profiles of DOX from DOX-loaded nanoparticles based on FCC (FCC-DOX). We used varying initial feed weight ratios of DOX to nanoparticles, ranging from 0.1:1.0 to 0.8:1.0. All of them showed an initial burst release phase and a sustained release phase: the entrapped DOX was released from 30.28 to 68.52% during 12 h, afterwards; the release rate was slow down. The DOX from loaded nanoparticles showed sustained release of about 97% (0.1:1) and 44% (0.8:1) respectively and the remaining 54% (0.8:1) of initial loading amount have not been released over 7 days. The initial burst release may be due to the DOX adsorbed on the shell of the nanoparticles. When the loading content is heavy, there will be relatively more DOX dissociated in the solution or absorbed on the surface of nanoparticles, thus increase the content of burst release. On the other hand, the mechanisms of slow release may involve the chitosan nanoparticles that had a rigid and hydrophobic core. This structure led to the migration of DOX which was strongly restricted, and slow release behavior was observed [22–25]. Furthermore, it may attribute to the strong hydrophobic interaction between FA segments and DOX.

**Fig. 6** In vitro release profiles of DOX from FCC nanoparticles with varying initial feed weight ratios of DOX to copolymer**Fig. 7** Cellular uptake efficiency of FCC and LCC nanoparticles by HeLa cells

3.6 In vitro cellular uptake of nanoparticles

The cellular uptakes of nanoparticles were quantitatively evaluated by FITC-labeled FCC and LCC nanoparticles and the measurement of fluorescence intensity. Figure 7 shows that cellular uptake efficiency of fluorescent FCC nanoparticles and fluorescent LCC nanoparticles depends on the concentration of nanoparticles suspension (0.005–0.1 µg/ml). As the concentration of nanoparticles suspension increased, the cellular uptake of FCC and LCC nanoparticles gradually increased. The concentration dependence maybe because nanoparticles could be transported through nonspecific receptor-mediated endocytosis. In addition, the cells treated with FCC nanoparticles exhibited higher cellular uptake efficiency than those treated with LCC nanoparticles, for all samples tested. The possible reason of the higher cell uptake efficiency of FCC nanoparticles is that the nanoparticles with FA are easier internalized into cells by FA receptor-mediated endocytosis than that of LCC nanoparticles [10–13].

Fluorescence images of FITC-FCC uptake by HeLa cells were presented in Fig. 8. The 1 h image of FITC-FCC showed cell periphery localization. Over the course of 4 h, abroad distribution of fluorescence in the cytosol were observed, which indicated FITC-FCC were indeed entering cell.

3.7 In vitro antitumor activity

Figures 9 and 10 shows the cell viability treated with FCC-DOX, DOX-loaded nanoparticles based on LCC (LCC-DOX) and free DOX at various DOX concentrations for various incubation times. The free nanoparticles show almost no effects on the cytotoxicity of cells. The viability of cells treated with FCC-DOX, LCC-DOX and free DOX decreased with increasing DOX concentration and incubation time. Folate modified carboxymethyl chitosan-DOX

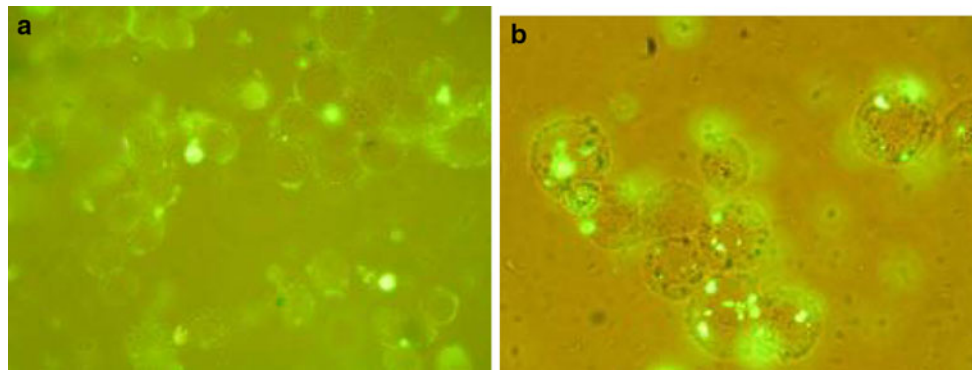


Fig. 8 Fluorescence microscopic images of HeLa cells incubated with FITC-FCC nanoparticles with a concentration of 0.2 mg/ml. **a** After 1 h incubation. **b** After 4 h incubation

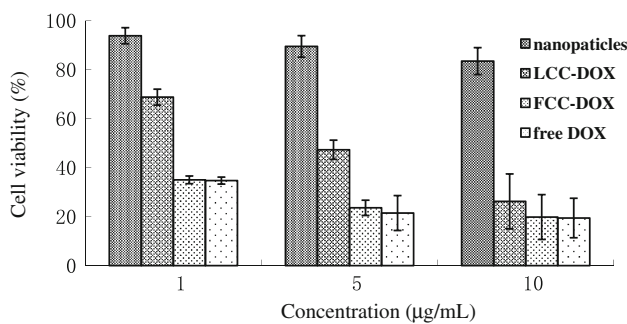


Fig. 9 Viability of Hela cells treated with the FCC-DOX, LCC-DOX, free DOX and the free nanoparticles at various DOX concentrations for 3 days

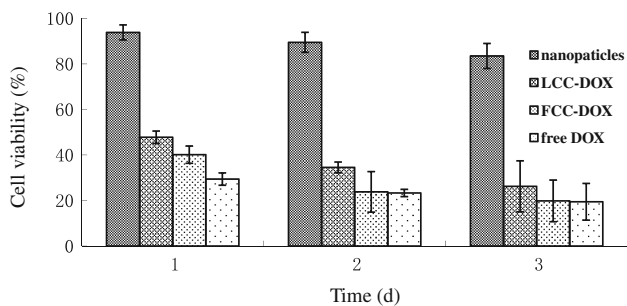


Fig. 10 Viability of Hela cells treated with the FCC-DOX, LCC-DOX, free DOX and the free nanoparticles at DOX concentration of 10 µg/ml for various days

and LCC-DOX showed slightly decreased cytostatic activity relative to the free DOX over the same concentration range. Since nanoparticles can only be internalized in the cells by the endocytosis process, rather than to the release of free drug in the cell culture medium which diffuse into the cells quickly as a small molecule. Furthermore, DOX was loaded into nanoparticles which might impede its release to the nucleus. When the drug content is 10 µg/ml after 3 days incubation, the cell viability for

LCC-DOX, FCC-DOX and free DOX is 26.22, 19.83 and 19.45%, respectively. It implies that the DOX is released from the nanoparticles inside the cells without losing cytotoxicity once nanoparticles are transported across the membrane due to endocytose. And DOX was released in a continuous way which conformed to release characteristic. In addition, FCC-DOX exhibit significantly more inhibitory activity than LCC-DOX because the FCC nanoparticles had higher cell uptake efficiency due to a specific interaction with Hela cells over-expressing the FA receptor via ligand-receptor recognition. This result indicates that FCC nanoparticles are potential carriers to deliver DOX into cells for the targeting therapy.

4 Conclusions

Carboxymethyl chitosan was modified by coupling with FA through the EDC-mediated reaction. Folate modified carboxymethyl chitosan is able to form nanoparticles via undergoing intra- and/or intermolecular association between folic acid moieties in aqueous environment. Nanoparticles have been used to solubilize hydrophobic drugs, such as DOX. And we found that the greater was the amount of DOX added the slower was sustained release. Folate modified carboxymethyl chitosan-DOX showed a comparable inhibition of the growth of cells to that of free DOX. Folate modified carboxymethyl chitosan nanoparticles can be used as a FA-receptor-targeted drug carrier for tumor-specific drug delivery.

Acknowledgment This work was supported by natural science foundation of shandong province of China (ZR2009CM071).

References

1. Hamidi M, Azadi A, Rafiei P. Hydrogel nanoparticles in drug delivery. *Adv Drug Deliv Rev.* 2008;60:1638–49.

2. Liu Z, Jiao Y, Wang Y, Zhou C, Zhang Z. Polysaccharides-based nanoparticles as drug delivery systems. *Adv Drug Deliv Rev.* 2008;60:1650–62.
3. Park JH, Kwon S, Lee M, Chung H, Kim JH, Kim YS, Park RW, Kim IS, Seo SB, Kwon IC, Jeong SY. Self-assembled nanoparticles based on glycol chitosan bearing hydrophobic moieties as carriers for doxorubicin: In vivo biodistribution and anti-tumor activity. *Biomaterials.* 2006;27:119–26.
4. Son YJ, Jang JS, Cho YW, Chung H, Park RW, Kwon IC, Kim IS, Park JY, Seo SB, Park CR, Jeong SY. Biodistribution and anti-tumor efficacy of doxorubicin loaded glycol-chitosan nanoaggregates by EPR effect. *J Control Release.* 2003;91:135–45.
5. Na K, Lee TB, Park KH, Shin EK, Lee YB, Cho HK. Self-assembled nanoparticles of hydrophobically-modified polysaccharide bearing vitamin H as a targeted anti-cancer drug delivery system. *Eur J Pharm Sci.* 2003;18:165–73.
6. Park JS, Han TH, Lee KY, Han SS, Hwang JJ, Moon DH, Kim SY, Cho YW. *N*-acetyl histidine-conjugated glycol chitosan self-assembled nanoparticles for intracytoplasmic delivery of drugs: endocytosis, exocytosis and drug release. *J Control Release.* 2006;115:37–45.
7. Zhao X, Li H, Lee RJ. Targeted drug delivery via folate receptors. *Expert Opin Drug Deliv.* 2008;5:309–19.
8. Leamon CP, Cooper SR, Hardee GE. Folate-liposome-mediated antisense oligodeoxynucleotide targeting to cancer cells: evaluation in vitro and in vivo. *Bioconjug Chem.* 2003;14:738–47.
9. Cho KC, Kim SH, Jeong JH. Folate receptor-mediated gene delivery using folate-poly(ethylene glycol)-poly(L-lysine) conjugate. *Macromol Biosci.* 2005;5:512–9.
10. Zhao HZ, Yung LYL. Selectivity of folate conjugated polymer micelles against different tumor cells. *Int J Pharm.* 2008;349:256–68.
11. Xiang GY, Wu J, Lu YH. Synthesis and evaluation of a novel ligand for folate-mediated targeting liposomes. *Int J Pharm.* 2007;356:29–36.
12. Park EK, Kim SY, Lee SB. Folate-conjugated methoxy poly(ethylene glycol)/poly(ϵ -caprolactone) amphiphilic block copolymeric micelles for tumor-targeted drug delivery. *J Control Release.* 2005;109:158–68.
13. Liang B, He ML, Xiao XP. Synthesis and characterization of folate-PEG-grafted-hyperbranched-PEI for tumor-targeted gene delivery. *Biochem Biophys Res Commun.* 2008;367:874–80.
14. Schroeder JE, Shweky I, Shmeeda H, Banin U, Gabizon A. Folate-mediated tumor cell uptake of quantum dots entrapped in lipid nanoparticles. *J Control Release.* 2007;124:28–34.
15. Mansouri S, Cuie Y, Winnik F, Shi Q, Lavigne P, Benderdour M, Beaumont E, Fernandes JC. Characterization of folate-chitosan-DNA nanoparticles for gene therapy. *Biomaterials.* 2006;27:2060–5.
16. Wan A, Suna Y, Li H. Characterization of folate-graft-chitosan as a scaffold for nitric oxide release. *Int J Biol Macromol.* 2008;43:415–21.
17. Cai S, Thati S, Bagby TR, Diab HM, Davies NM, Cohen MS, Forrest ML. Localized doxorubicin chemotherapy with a biopolymeric nanocarrier improves survival and reduces toxicity in xenografts of human breast cancer. *J Control Release.* 2010;146:212–8.
18. Lee H, Ahn CH, Park TG. Poly[lactic-co-(glycolic acid)]-grafted hyaluronic acid copolymer micelle nanoparticles for target-specific delivery of doxorubicin. *Macromol Biosci.* 2009;9:336–42.
19. Xiong XB, Ma ZS, Lai R, Lavasanifar A. The therapeutic response to multifunctional polymeric nano-conjugates in the targeted cellular and subcellular delivery of doxorubicin. *Biomaterials.* 2010;32:757–68.
20. Tan YL, Liu CG. Self-aggregated nanoparticles from linoleic acid modified carboxymethyl chitosan: synthesis, characterization and application in vitro. *Colloids Surf B Biointerfaces.* 2009;69:178–82.
21. Liu CG, Desai KGH, Chen XG, Park HJ. Linolenic acid-modified chitosan for formation of self-assembled nanoparticles. *J Agric Food Chem.* 2005;53:437–41.
22. Tian Z, Wang M, Zhang AY. Preparation and evaluation of novel amphiphilic glycopeptide block copolymers as carriers for controlled drug release. *Polymer.* 2008;49:446–54.
23. An XY, Yang J, Wang M. Preparation of chitosan–gelatin scaffold containing tetrandrine-loaded nano-aggregates and its controlled release behavior. *Int J Pharm.* 2008;28:257–64.
24. Zhang J, Chen XG, Liu CS, Park HJ. Investigation of polymeric amphiphilic nanoparticles as antitumor drug carriers. *J Mater Sci Mater Med.* 2009;20:991–9.
25. Sheikh FA, Barakat NAM, Kanjwal MA, Aryal S, Khil MS, Kim HY. Novel self-assembled amphiphilic poly(ϵ -caprolactone)-grafted-poly(vinyl alcohol) nanoparticles: hydrophobic and hydrophilic drugs carrier nanoparticles. *J Mater Sci Mater Med.* 2009;20:821–31.